Journal of Electrochemistry

Volume 22
Issue 2 *Special issue of Electrocatalyst and Electrocatalysis in Fuel Cells(Editor: Professor WEI Zi-dong)*

2016-04-28

# Recycling MF Solid Waste into Mesoporous Nitrogen-doped Carbon with Iron Carbide Complex in Graphitic Layers as An efficient Catalyst for Oxygen Reduction Reaction

Can-yun ZHAO

Lin HUANG

Yong YOU

Ying-fang YAO

Xiao-gang SU

Hong WAN

Jian-guo LIU
*College of engineering and Applied sciences, Nanjing University, Nanjing 210093, China;Eco-materials renewable Energy Research Center, Nanjing University, Nanjing 210093, China;Kunshan Innovation Institute of Nanjing University, Kunshan 215347, China;Suzhou High-tech Institute of Nanjing University, Suzhou 215123, China;*, jianguoliu@nju.edu.cn

*See next page for additional authors*

## Recommended Citation

Can-yun ZHAO, Lin HUANG, Yong YOU, Ying-fang YAO, Xiao-gang SU, Hong WAN, Jian-guo LIU, Cong-ping WU. Recycling MF Solid Waste into Mesoporous Nitrogen-doped Carbon with Iron Carbide Complex in Graphitic Layers as An efficient Catalyst for Oxygen Reduction Reaction[J]. *Journal of Electrochemistry*, 2016 , 22(2): 176-184.
DOI: 10.13208/j.electrochem.151145
Available at: https://jelectrochem.xmu.edu.cn/journal/vol22/iss2/8

This Article is brought to you for free and open access by Journal of Electrochemistry. It has been accepted for inclusion in Journal of Electrochemistry by an authorized editor of Journal of Electrochemistry.

# Recycling MF Solid Waste into Mesoporous Nitrogen-doped Carbon with Iron Carbide Complex in Graphitic Layers as An efficient Catalyst for Oxygen Reduction Reaction


## Authors

Can-yun ZHAO, Lin HUANG, Yong YOU, Ying-fang YAO, Xiao-gang SU, Hong WAN, Jian-guo LIU, and Cong-ping WU

## Corresponding Author(s)

Jian-guo LIU(jianguoliu@nju.edu.cn)



This article is available in Journal of Electrochemistry: https://jelectrochem.xmu.edu.cn/journal/vol22/iss2/8

**DOI**: 10.13208/j.electrochem.151145 **Artical ID**:1006-3471(2016)02-0176-09
**Cite this**: *J. Electrochem.* **2016**, *22*(2): 176-184 **Http**://electrochem.xmu.edu.cn

# 三聚氰胺甲醛树脂废弃物制备氧还原电催化剂研究

赵灿云[1,2],黄 林[1,2,3],尤 勇[1,2],姚颖方[1,2,3],
苏小钢[1,2],万 红[1,2],刘建国[1,2,3,4*],吴聪萍[1,2,3]
(1. 南京大学现代工程与应用科学学院, 江苏 南京 210093;
2. 南京大学物理学院环境材料与再生能源研究中心, 江苏 南京 210093;
3. 南京大学昆山创新研究院, 江苏 昆山 215347; 4. 南京大学(苏州)高新技术研究院, 江苏 苏州 215123)

**摘要:** 在燃料电池阴极催化剂的研究中,FeN*x*/C 材料与目前广泛应用在燃料电池中的 Pt 基催化剂相比, 不仅价格低廉,而且表现出良好的氧还原催化活性. 尽管如此,设计合成性能高、成本低的 FeN*x*/C 催化剂仍面临巨大挑战. 在此,作者提出废物利用的方法,以三聚氰胺甲醛树脂固体废物为前驱体,合成了具备介孔结构和较大的比表面积的非贵金属催化剂. 经酸性条件半电池测试,这种电催化剂的氧还原催化活性接近 5%商业 Pt/C 性能. 本文工作为三聚氰胺甲醛树脂固体废弃物处理提供了新思路.

**关键词:** 三聚氰胺甲醛树脂;质子交换膜燃料电池;氧还原;FeN*x*/C;催化剂;废物利用
**中图分类号:** TM91; O646 **文献标识码:** A

随着新能源的发展, 燃料电池及其他电池设备被认为有望代替传统的化石能源[1-2]. 但是,阴极氧还原(Oxygen Reduction Reaction,ORR)活性差,严重阻碍了燃料电池发展, 因此合成高活性的电催化剂受到研究者关注[3-5]. 目前,贵金属材料(如 Pt 及其合金) 制备阴极电催化剂具有高氧还原活性[6-7],但 Pt 稀缺且昂贵阻碍其应用,因而使用价格低廉的非铂材料代替 Pt 材料成为当前研究热点[8-11]. 目前,已有多种非铂催化剂被广泛报道,金属氧化物[12]、有机金属配合物[13]、杂原子碳材料[14]、硫属化合物[15]以及仿生材料[16]均被证明有良好的氧还原活性. 尽管如此,这些材料用在燃料电池上仍存在价格昂贵、性能不稳定等缺点.

理论上, 催化剂的高比表面积有助于提高 ORR 性能,如薄膜纳米片[3,17-19],其高比表面积暴露更多的二维空间催化点提高 ORR 性能. 研究还发现,纳米级孔隙度、高传质及有效载量对 ORR 性能也有一定影响[20]. 基于此种思路,碳纳米管(CNTs)、碳纳米纤维(CNFs)以及石墨烯等氮掺杂碳催化剂受到研究者重视[21],其中一些研究者将注意力集中在氮金属共掺杂碳催化剂体系[10]. 从最新报道来看,从可持续发展角度, 使用生物质碳作为前驱体,实现氮和金属共掺杂,不仅价格低廉,且避免有害无机物和有机化合物的使用[22-23]. 和无掺杂的碳材料相比, 这种材料表现出 N 型半导体和金属的特性,且具有更好的电子迁移率[24-25]. 越来越多的研究者在朝此方向尝试,比如前驱体选择马齿苋[26]、三聚氰胺奶粉[27]、猪血[28]、大豆[29]及鲤鱼[30]等生物质材料,这些材料含氮的大分子[31]或小分子[32]有助于电催化剂 ORR 性能的提高.

三聚氰胺甲醛树脂(Melamine-Formaldehyde Resin, MF)被大量用作仿瓷餐具的加工制造,废弃仿瓷餐具的处理挑战巨大. 作者利用 MF 固体废弃物作为前驱体合成 FeN*x*/C 材料, 即 MCFes 材料(M-MF, C-碳粉(BP2000),Fe 铁),选择 MF 固体废弃物的具体优势包括:1)MF 固体废弃物回收利用,不仅环境友好且提供丰富的碳源和氮源;2)利用 MF 废弃物制备的催化剂具有明显的介孔结构

收稿日期: 2015-01-27, 修订日期: 2015-02-06 * 通讯作者, Tel: (86-25)83621219, E-mail: jianguoliu@nju.edu.cn
国家自然科学基金项目(No. 21476104)、江苏省自然科学基金杰出青年基金(No. BK20150009)、江苏省自然科学基金青年基金项目(No. BK20150396)、江苏省软科学研究项目(No. BR2015009)及江苏省苏州市纳米技术专项(No. ZXG2013029)资助

及较高的比表面积;3)合成的 FeN$x$/C 材料在酸性介质的催化活性与 5%商业 Pt/C 接近.

# 1 实　验

## 1.1 试剂与仪器

活性碳 Vulcan BP2000($\phi$ = 12 nm),MF 固体废弃物为食堂中使用过的三聚氰胺甲醛树脂筷子,5% Nafion 溶液(质量分数,下同,杜邦公司),5%商业 Pt/C (Johnson Matthey 公司),$FeCl_3\cdot 6H_2O$、$HClO_4$ 购于国药集团化学试剂公司, 压缩氧气和氨气购自南京天泽气体.

Rigaku D/MAX-Ultima III 型 X 射线衍射仪(荷兰 Philip 公司),激发光源 Cu-$K_\alpha$ 辐射($\lambda$ = 0.15406 nm),扫描角度 10°~80°,扫描速率为 10°·min$^{-1}$; 英国 VG Scientific ESCA Lab MK-II 扫描 X 射线光电子能谱(XPS)仪,激发光源 Mg-$K_\alpha$; 新星 NanoSEM230 扫描电子显微镜 (Scanning Electron Microscopy,SEM,FEI 公司);JEM-200CX 高倍率透射电子显微镜 (Transmission Electron Microscopy, TEM,日本 JEOL 公司);美国 Micromeritics Tristar 3000 氮气吸脱附分析仪, 测试温度 77 K; 德国 Netzsch 公司 STA449F3 型热分析仪.

## 1.2 样品制备与测试

1)原料制备

MF 废弃物预处理:将 MF 固体废弃物餐具清洗后粉碎成颗粒状, 所得毫米级颗粒物在管式炉中 $N_2$ 气氛下以 5 ℃·min$^{-1}$ 的速率升温至 250 ℃,烧结 1 h. 自然冷却后放入 $H_2SO_4$ (1 mol·L$^{-1}$,50 mL)中酸洗 24 h,产物过滤后在 80 ℃ 烘箱干燥 8 h,命名为 M250.

MCFes 制备:将预处理产物与 $FeCl_3\cdot 6H_2O$ 及碳黑混合后球磨 6 h. 混合后的产物在管式炉($N_2$ 气氛)中以 5 ℃·min$^{-1}$ 的速率升温至 950 ℃,并在此高温烧结 1 h.此过程中铁元素扩散到碳基体,也即 MF 固体废弃物、碳黑及 $FeCl_3\cdot 6H_2O$ 经高温处理形成多孔的 FeN$x$/C 催化剂. 实验中选择预处理产物、碳黑、Fe 的比例分别为 10/10/1、10/10/2、10/10/4,所得产物命名为 MCFe-10/10/$X$($X$ 代表 Fe 不同比例). 为做对照, 将 10/10/2 比例在 $NH_3$ 气氛下以同种烧结条件处理, 所得产物标示为 NMCFe-10/10/X.

2)材料电化学表征

循环伏安(CV)测试、ORR 测试、$H_2O_2$ 产率测试均在 0.1 mol·L$^{-1}$ $HClO_4$ 中使用旋转环盘电极(Rotating Ring-Disk Electrode,RRDE)室温下完成. Pt 电极、可逆氢电极(RHE)、旋转环盘电极分别用作辅助电极、参比电极、工作电极. 旋转环盘工作电极(GC,$\phi$ = 5 mm)表面涂层墨汁状催化剂. 催化剂配制过程如下:10 mg 催化剂、96 μL Nafion、350 μL 乙醇混合,冰浴超声 40 min,催化剂室温干燥载量 204 μg·cm$^{-2}$. 测试前,向 0.1 mol·L$^{-1}$ $HClO_4$ 的溶液分别通入 $O_2$ 及 $N_2$ 30 min 使溶液气体过饱和. CV 测试时,在 1.2~0 V(VS. RHE)下以 50 mV·s$^{-1}$ 速率扫描 10 周, 待 CV 性能稳定后在 900 r·min$^{-1}$ 下以 10 mV·s$^{-1}$ 扫速测试 ORR 性能. 电流在均一的几何化电极上进行(ca. 0.19625 cm$^2$).

3)单电池测试

Nafion 膜(211 膜,有效面积 1.0 cm$^2$)夹在涂有催化剂的碳纸间制备膜电极 MEA (Membrane Electrode Assembly). 阴极催化剂配制:20 mg 样品 MCFe-10/10/2、100 μL Nafion、350 μL 去离子水及 350 μL 乙醇冰浴超声混合 20 min. 使用静电纺丝仪将催化剂喷在碳纸上,载量为 4 mg·cm$^{-2}$,干燥后催化剂与 Nafion 的比例为 2/1. 阳极催化剂使用 60% Pt/C,干燥后载量为 0.2 $mg_{pt}\cdot cm^{-2}$ 且 Nafion 达 33%. 测试时, 膜电极和流场契合夹在 PTFE(45 mm × 45 mm,厚度 200 nm)间,热电偶插在两石墨片间获得所需温度.

燃料电池极化曲线在燃料电池测试系统(Model 850e,Scribner Associates Inc.) 上完成. 100%相对湿度电池测试温度 80 ℃,氢气流速 300 sccm,氧气流速 800 sccm,测试在无背压状态完成.

# 2 结果与讨论

## 2.1 MCFes 合成过程

图 1 为 MCFes 合成过程,样品制备包括 250 ℃ 预处理和 950 ℃ 高温热处理两个热解过程. 选择 250 ℃ 预处理的原因是样品在此温度前失水及不稳定物质分解,而在此温度后样品组分发生变化,质量大幅度下降(见附文图 S1D).

## 2.2 MCFes 结构和表面特征

样品 MCFes 氮吸脱附等温曲线可知,3 种样品均具有较大的比表面积(图 2A),IV 型等温线表明样品为介孔材料(图 2B). 表 1 列出不同样品比表面积大小和杂质原子含量, 样品 MCFe-10/10/2 最大比表面积可达 780.7 m$^2$·g$^{-1}$. 附文图 S2 为 NMCFe-10/10/2 氮的吸脱附及孔径分布曲线, 该样品比表面积 533.7 m$^2$·g$^{-1}$. 结果显示,合适的铁含量为

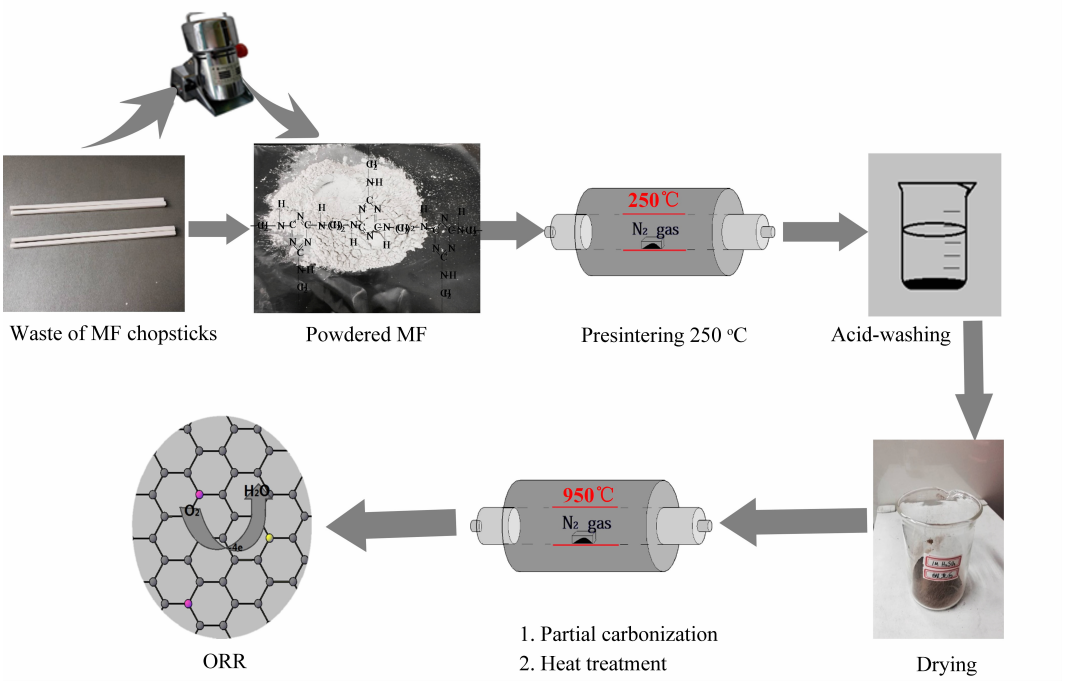


图 1　样品 MCFes 合成示意图

Fig. 1　Schematic procedure for the fabrication of MCFes

催化剂 ORR 性能提供必要的杂原子. 已有报道指出,传质性能很大程度上取决于孔隙结构及分布,高比表面积材料将暴露更多活性位点,一般来说,中孔和大孔证明能够有效的运输 ORR 相关物质($O_2$、$H^+$、$OH^-$、$H_2O$)[33-35]. 因此,高表面积及合适的中/大孔隙有助于提高 ORR 性能. 实验制备的 MCFe-10/10/2 催化剂具有高比表面积和合适的中/大孔隙结构,同样表现出良好的 ORR 性能.

样品 MCFe-10/10/2XPS 分析谱图示于图 2C,测得催化剂碳原子比例为 83.81%、氧原子比例为 13.52%、氮原子比例为 1.49%(图 2C 内插图). 样品 N1s 高分辨频谱分峰后可得到 4 种 N (图 2D):氧化吡啶氮(403.1 eV,N1)、石墨氮(401.2 eV,N2)、吡咯氮(400.1 eV,N3)和吡啶氮(397.5 eV,N4)[26,36-37]. 图 2D 中 C1s 的光谱在 284.4、285.2、286.1、289.1 eV 存在 4 个峰值. 其中,286.1 eV 与 C—N 相一致[26],表明碳框架完成氮掺杂(由附文图 S3 中可见其他样品的 C1 分峰和 N1 分峰). 实验发现, 经高温处理,样品所掺杂氮含量和 $Fe^{3+}$ 有关. 氨气下掺氮处理得到 NMCFe-10/10/2 氮含量最高, 而性能低于 MCFe-10/10/2,说明氮含量适中为宜(表 1). 此外, 样品 MCFe-10/10/2 石墨层表面中检测到很强的 Fe 信号,这些 Fe 信号来自形成的 $Fe_xC$(图 2F).

图 3A 的 XRD 图用来表征 FeN*x*/C 的掺杂状态. 样品 MCFes 在 24.9°和 44.0°峰值与涡轮层碳(002)和(100)点阵平面相对应[38]. 众所周知,碳的石墨化可提高电催化剂电子电导性和耐腐蚀性[39]. 实验样品 MCFe-10/10/2 出现很强的 $Fe_3C$(JCPDS No. 35-0772)峰值(附文图 S4). 此外,30°、35.7°、56.5°和 62.9°峰与 $Fe_3O_4$(JCPDS card No. 65-3107)对应, 说明酸洗后样品杂质基本除净且样品中 Fe 被空气中氧气氧化. 此外,50.3°峰和 $CFe_{15.1}$(JCPDS card No. 52-0512) 对应. 说明样品高温处理后形成 $Fe_xC$, 并以 $CFe_{15.1}$ 和 $Fe_3C$ 存在, 数据结果和 EDS 图像及 XPS 分析一致.

图 3B 和附图 1A 中 SEM 照片说明,M250 酸洗形成有助包覆碳黑及 Fe 原子的多孔结构. 经 XRD 和 XPS 分析, 高温烧结形成的 FeN*x*/C 与 M250 分解的 N 原子均匀络合. 由 TEM 结构表征可知,样品表面存在典型的介孔结构,且纳米 Fe 颗粒均匀分布在石墨层间(图 3C-D),形成的多孔结构空隙范围在 40 nm ~ 200 nm 间. 与附文图 5 对比, 样品 MCFe-10/10/1 中 Fe 含量过少, 而样品 MCFe-10/10/4 的 Fe 过多产生团聚, 表明形成 FeN*x*/C 结构 10/10/2 比例较为适中. 从 TEM 照片

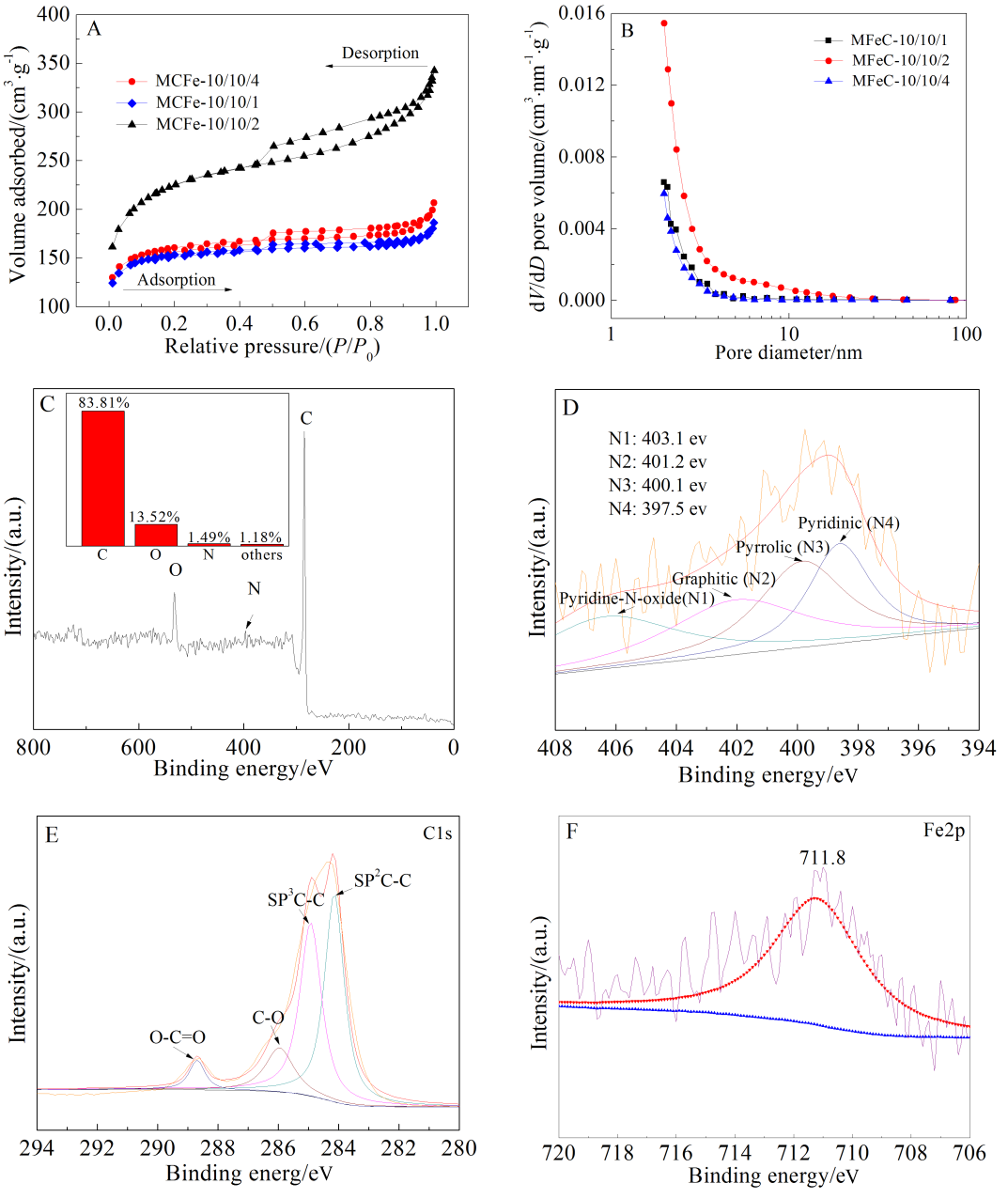


图 2　A. 样品 MCFes 氮气吸脱附曲线;B. 样品 MCFes 孔径分布图;C. 样品 MCFe-10/10/2 的 XPS 全谱分析（内图为对应碳、氮、氧等元素比例);D-F. 样品 MCFe-10/10/2 N1s、C1s、Fe2p XPS 谱图

Fig. 2　A. Nitrogen adsorption/desorption isotherms of MCFes; B. Corresponding pore size distribution curves; C. XPS survey of the MCFe-10/10/2 (the inset: chart showing the percentages of carbon, nitrogen, oxygen and other elements according to XPS data); D-F. XPS data for the N1s, C1s and Fe2p regions of MCFe-10/10/2

还可看出,Fe 颗粒和石墨层接触完全,这说明石墨层约束金属纳米颗粒，可提高金属颗粒和导电碳层之间的接触界面，抑制金属纳米颗粒的溶解和集聚,从而提高电化学活性和稳定性[40].

## 2.3　酸性条件下 MCFes 电催化剂 ORR 性能

使用旋转圆盘电极测试 ORR 性能,结果如图 4 所示. 图 4A 将 MCFes 和 5%商业 Pt/C 催化剂对比. 样品 MCFe-10/10/2（0.95 V）起始电位比样品 MCFe-10/10/1(0.68 V)和样品 MCFe-10/10/4(0.83 V)起始电位提高很多,和 5%商业 Pt/C(0.96 V)对比，此催化剂仅低 0.1 V. 此外，与样品 NM-CFe-10/10/2 及其他非贵金属催化剂(附图 S6、附表

表 1 样品氮气吸脱附分析和 XPS 分析得到的各参数

Tab. 1 Summary of textural parameters obtained from nitrogen adsorption analysis and chemical compositions from XPS analysis

| Sample | $S_{BET}$/ ($m^2 \cdot g^{-1}$) | Total pore volume/ ($cm^3 \cdot g^{-1}$) | Micro pore volume/ ($cm^3 \cdot g^{-1}$) | Chemical composition/%(by atom) | | | | | | |
|---|---|---|---|---|---|---|---|---|---|---|
| | | | | C | O | N | N1 | N2 | N3 | N4 |
| MCFe-10/10/1 | 546.1 | 0.2952 | 0.1779 | 84.88 | 13.83 | 0.10 | 29.3 | 24.7 | 18.6 | 27.4 |
| MCFe-10/10/2 | 780.7 | 0.2678 | 0.1790 | 83.81 | 13.52 | 1.49 | 22.5 | 25.9 | 23.8 | 27.8 |
| MCFe-10/10/4 | 521.0 | 0.4908 | 0.1883 | 85.29 | 12.20 | 0.17 | 23.8 | 18.7 | 18.7 | 38.8 |
| NMCFe-10/10/2 | 533.7 | 0.4208 | 0.0875 | 83.21 | 13.28 | 2.72 | 27.3 | 16.8 | 23.9 | 32.0 |

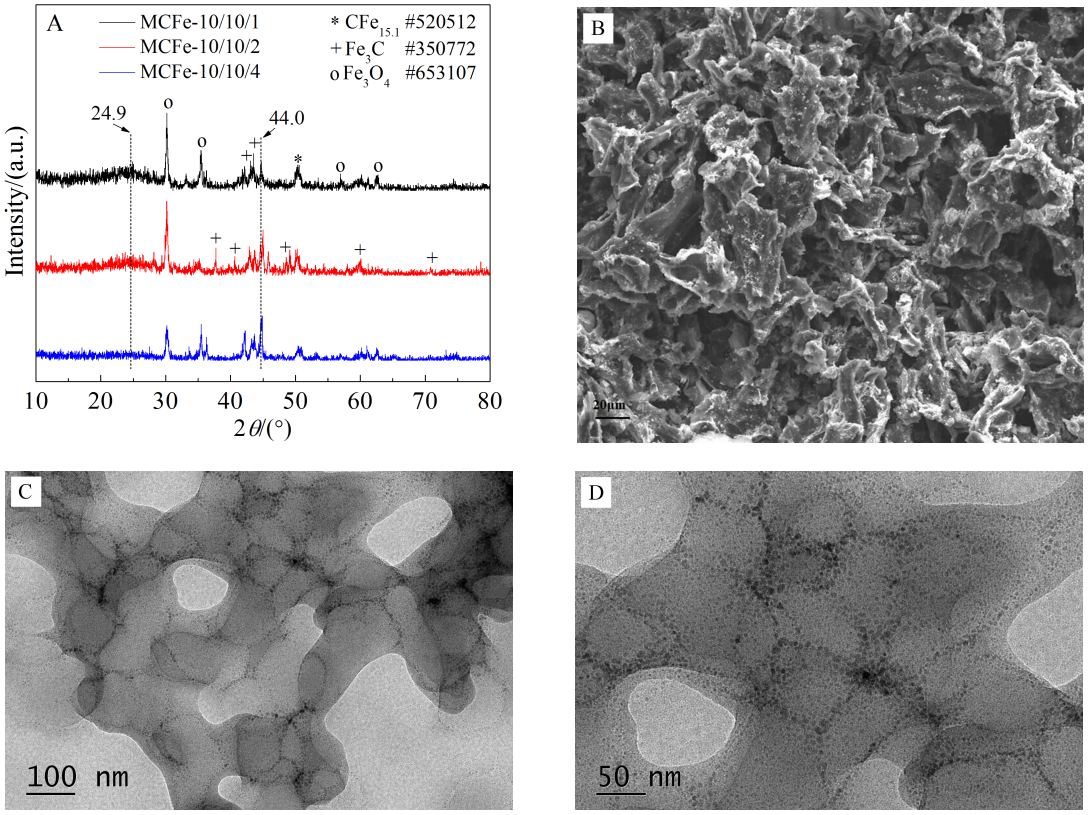


图 3 A. 样品 MCFes X 射线衍射谱图;B. 样品 M250 扫描电镜照片;C-D. 样品 MCFe-10/10/2 透射电镜照片

Fig. 3 A. Powder XRD patterns of MCFes over the 2$\theta$ range of 10° ~ 80°; B. SEM image of M250; C-D. TEM images of MCFe-10/10/2

1)对比,MCFe-10/10/2 均表现出很高的 ORR 催化活性,造成这种情况原因主要是不同 Fe 含量导致样品比表面积、空隙大小及活性位点不同,大比表面积和介孔结构有利于活性位点的暴露从而提高 ORR 性能. 研究发现,溶液和催化剂的传质决定极限电流大小. 如果催化剂表面比周围扩散快,扩散极限电流仅取决于电极旋转速率与催化剂种类关系不大[42]. 由此可知,同转速下 MCFe-10/10/2 极限电流密度扩散阻力比其他样品小. 其他研究者前期工作中亦有报道[43],铁掺杂有助于将惰性氮变成有助提高 ORR 性能的活性氮,也就是说可增强氧还原活性位点提高催化活性. 本文不仅优化了 Fe 含量,而且制备的催化剂具有高比表面积、介孔结构,同时形成了活性的 $Fe_xC$ 结构.

图 4B 给出 MCFe-10/10/2 不同转速下的 ORR 极化曲线. 图线表明,样品的极限电流密度随转速的增加而增加,而样品的起始电位不变. Koutecky-Levich(K-L)动力学方程表明[44],ORR 一阶反应动力学和溶氧的浓度有关. 从图 4C 看出存在良好的线性关系, 且在 0.05 ~ 0.55 V 可逆氢电极(vs.

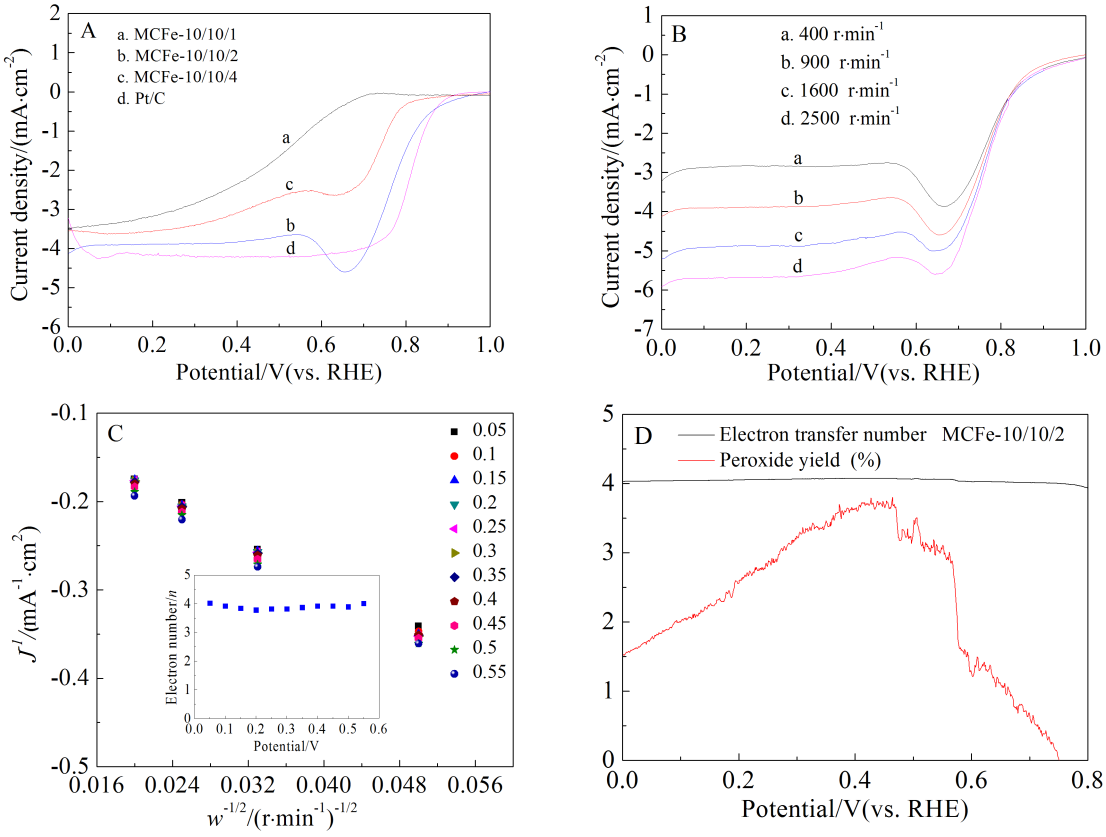


图 4　A. MCFes 和 Pt/C 在 0.1 mol·L$^{-1}$ $HClO_4$ 溶液中 900 r·min$^{-1}$ 转速下的 ORR 极化曲线;B. 样品 MCFe-10/10/2 不同转速下的 ORR 极化曲线;C. 样品 MCFe-10/10/2 的 K-L 图(内图为根据 K-L 方程计算的电子转移数);D. 900 r·min$^{-1}$ 转速下旋转环盘电极测得的双氧水产率及电子转移数

Fig. 4　A. ORR polarization curves for MCFes and 5% Pt/C in 0.1 mol·L$^{-1}$ $HClO_4$ solution at a rotation rate of 900 r·min$^{-1}$; B. Linear sweep voltammograms for oxygen reduction on the MCFe-10/10/2 catalyst in 0.1 mol·L$^{-1}$ $HClO_4$ at various rotation speeds with a scan rate of 10 mV·s$^{-1}$; C. K-L plots for the ORR in $O_2$-saturated 0.1 mol·L$^{-1}$ $HClO_4$ solution for MCFe-10/10/2 (the inset is the electron number calculated from K-L plots); D. Hydrogen peroxide ($H_2O_2$) yield obtained from RRDE curves for the MCFe-10/10/2 in 0.1 mol·L$^{-1}$ $HClO_4$ with a scan rate of 10 mV·s$_{-1}$ at a rotation speed of 900 r·min$^{-1}$ and the electron transfer number as a function of potential

RHE)测试中,电子转移数 $n$ 在 3.8 ~ -4.3 之间,说明样品 MCFe-10/10/2 的 ORR 催化完成四电子还原过程. 为验证该结论,作者在旋转环盘电极 0.001 ~ 0.800 V(vs. RHE)范围内测试,得样品电子转移数在 3.93 ~ 4.07,两者结论一致,均说明 ORR 过程中四电子转移为主导. 此外,环形电极 $H_2O_2$ 产率小于 3.8%(图 4D),而 0.055 ~ 0.900 V(vs. RHE)商业 Pt/C 电子转移数在 3.90 ~ 3.97 之间,环形电极的 $H_2O_2$ 产率低于 4.2%[41],所制备的 MCFe-10/10/2 催化剂已趋近商业 Pt/C 的电催化性能.

MCFe-10/10/2 催化剂具有良好的 ORR 性能,为进一步研究,作者进行了全电池测试(图 5). 质子交换膜燃料电池开路电压(Open Circuit Voltage, OCV)达 0.63 V,和商业 Pt/C 阴极 0.77 V 的开路电压还有一定距离 [44]. 全电池的最高功率密度为 180 mw·cm$^{-2}$, 在非贵金属催化剂领域特别是废物利用方面电池性能优越. 将 MF 固体废弃物合成非铂催化剂并且用于质子交换膜燃料电池, 还是首次报道.

## 3　结　论

目前研究显示, 非贵金属催化剂在金属-空气电池和燃料电池方面很有发展潜力. 作者利用三聚氰胺甲醛树脂废弃物制备非铂催化剂, 原料成本低、方法简单且具有良好的电催化性能,为回收处理含氮固体废弃物提供了新思路. 所制备的 MCFe 催化剂中的纳米结晶 $Fe_xC$ 微粒被封装在 N

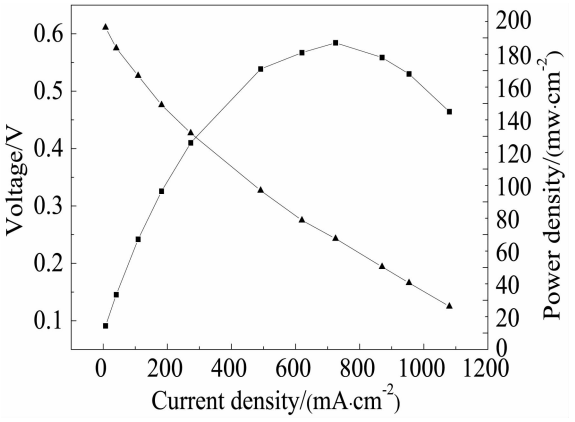


图 5 质子交换膜燃料电池全电池性能

Fig. 5 Acidic PEMFC performance at 80 ℃ using MCFe-10/10/2 (4 mg·cm$^{-2}$) as the cathode catalyst and Pt/C (60%, JM 0.2 mgpt·cm$^{-2}$) as the anode catalyst. Hydrogen was supplied to the anode at a flow rate of 300 sccm. Dry oxygen was supplied to the cathode at a flow rate of 800 sccm.

介孔结构的掺杂骨架内，具有高比表面积. 其中，样品 MCFe-10/10/2 酸性条件下性能和 5%商业 Pt/C 相接近，同时在质子交换膜燃料电池全电池上表现出优良性能.

MF 固体废弃物作为前驱体提供丰富的氮源，而在实际生产生活中，含氮固体废弃物不止 MF 一种，例如脲醛树脂、聚氨酯等制备的塑料材料均含氮元素，基于此思路，制备非贵金属催化剂可以从氨基树脂和其他含氮塑料中选择前驱体. 随着研究的不断深入，回收利用固体废弃物将不会再是难题.

**附文**

附文请在《电化学》网站下载：http://electrochem.xmu.edu.cn.

## 参考文献(References)：

[1] Bruce P G, Hardwick L J, Abraham K M. Lithium-air and lithium-sulfur batteries[J]. Mrs Bulletin, 2011, 36(7): 506-512.

[2] Winter M, Brodd R J. What are batteries, fuel cells, and supercapacitors[J]. Chemical Reviews, 2004, 104(10): 4245-4269.

[3] Debe M K. Electrocatalyst approaches and challenges for automotive fuel cells[J]. Nature, 2012, 486(7401): 43-51.

[4] Liang Y Y, Li Y G, Wang H L, et al. $Co_3O_4$ nanocrystals on graphene as a synergistic catalyst for oxygen reduction reaction[J]. Nature Materials, 2011, 10(10): 780-786.

[5] Xiao M L, Zhu J B, Feng L G, et al. Meso/macroporous nitrogen-doped carbon architectures with iron carbide encapsulated in graphitic layers as an efficient and robust catalyst for the oxygen reduction reaction in both acidic and alkaline solutions[J]. Advanced Materials, 2015, 27(15): 2521-2527.

[6] Tang Q E, Jiang L H, Qi J, et al. One step synthesis of carbon-supported Ag/$MnyO_x$ composites for oxygen reduction reaction in alkaline media[J]. Applied Catalysis B-Environmental, 2011, 104(3/4): 337-345.

[7] Li Y J, Li Y J, Zhu E B, et al. Stabilization of high-performance oxygen reduction reaction Pt electrocatalyst supported on reduced graphene oxide/carbon black composite [J]. Journal of The American Chemical Society, 2012, 134 (30): 12326-12329.

[8] Levy R B, Boudart M. Platinum-like behavior of tungsten carbide in surface catalysis[J]. Science, 1973, 181(4099): 547-549.

[9] Guo S J, Sun S H. FePt nanoparticles assembled on graphene as enhanced catalyst for oxygen reduction reaction[J]. Journal of The American Chemical Society, 2012, 134 (5): 2492-2495.

[10] Wu G, More K L, Johnston C M, et al. High-performance electrocatalysts for oxygen reduction derived from polyaniline, iron, and cobalt[J]. Science, 2011, 332(6028): 443-447.

[11] Lefevre M, Proietti E, Jaouen F. Iron-based catalysts with improved oxygen reduction activity in polymer electrolyte fuel cells[J]. Science, 2009, 324(5923): 71-74

[12] Wu Z S, Yang S B , Sun Y, et al. 3D nitrogen-doped graphene aerogel-supported $Fe_3O_4$ nanoparticles as efficient eletrocatalysts for the oxygen reduction reaction[J]. Journal of The American Chemical Society, 2012, 134 (22): 9082-9085.

[13] Thorum M S, Yadav J, Gewirth A A. Oxygen reduction activity of a copper complex of 3,5-diamino-1,2,4-tria zole supported on carbon black[J]. Angewandte Chemie International Edition, 2009, 48(1): 165-167.

[14] Jaouen F, Herranz J, Lefevre M, et al. Cross-laboratory experimental study of non-noble-metal electrocatalysts for the oxygen reduction reaction[J]. ACS Applied Materials & Interfaces, 2009, 1(8): 1623-1639.

[15] Cheng F Y, Su Y, Liang J, et al. $MnO_2$-based nanostructures as catalysts for electrochemical oxygen reduction in alkaline media[J]. Chemistry of Materials, 2010, 22(3): 898-905.

[16] Cracknell J A, Vincent K A, Armstrong F A. Enzymes as working or inspirational electrocatalysts for fuel cells and

electrolysis[J]. Chemical Reviews, 2008, 108(7): 2439-2461.

[17] Yang W, Fellinger T P, Antonietti M. Efficient metal-free oxygen reduction in alkaline medium on high-surface-area mesoporous nitrogen-doped carbons made from ionic liquids and nucleobases[J]. Journal of The American Chemical Society, 2011, 133(2): 206-209.

[18] Parvez K, Yang S B, Hernandez Y, et al. Nitrogen-doped graphene and its iron-based composite as efficient electrocatalysts for oxygen reduction reaction[J]. ACS Nano, 2012, 6(11): 9541-9550.

[19] Wang J J, Zhu M Y, Outlaw R A, et al. Synthesis of carbon nanosheets by inductively coupled radio-frequency plasma enhanced chemical vapor deposition[J]. Carbon, 2004, 42(14): 2867-2872.

[20] Titirici M M, White R J, Falco C, et al. Black perspecti ves for a green future: Hydrothermal carbons for environment protection and energy storage [J]. Energy & Environmental Science, 2012, 5(5): 6796-6822.

[21] Tang Y F, Allen B L, Kauffman D R, et al. Electrocatalytic activity of nitrogen-doped carbon nanotube cups [J]. Journal of The American Chemical Society, 2009, 131(37): 13200-13201.

[22] Su D S. The use of natural materials in nanocarbon synthesis[J]. ChemSuschem, 2009, 2(11): 1009-1020.

[23] Raymundo-Pinero E, Cadek M, Beguin F. Tuning carbon materials for supercapacitors by direct pyrolysis of seaweeds[J]. Advanced Functional Materials, 2009, 19(7): 1032-1039.

[24] Jafri R I, Rajalakshmi N, Ramaprabhu S. Nitrogen-doped multi-walled carbon nanocoils as catalyst support for oxygen reduction reaction in proton exchange membrane fuel cell[J]. Journal of Power Sources, 2010, 195(24): 8080-8083.

[25] Zhou Y K, Neyerlin K, Olson T S, et al. Enhancement of Pt and Pt-alloy fuel cell catalyst activity and durability via nitrogen-modified carbon supports[J]. Energy & Environmental Science, 2010, 3(10): 1437-1446.

[26] Gao S Y, Geng K, Liu H Y, et al. Transforming organic-rich amaranthus waste into nitrogen-doped carbon with superior performance of the oxygen reduction reaction[J]. Energy & Environmental Science, 2015, 8(1): 221-229

[27] Zhao H, Hui K S, Hui K N. Synthesis of nitrogen-doped multilayer graphene from milk powder with melamine and their application to fuel cells[J]. Carbon, 2014, 76: 1-9.

[28] Guo C Z, Liao W L, Li Z B, et al. Exploration of the catalytically active site structures of animal biomass-modified on cheap carbon nanospheres for oxygen reduction reaction with high activity, stability and methanol-tolerant performance in alkaline medium[J]. Carbon, 2015, 85: 279-288.

[29] Zhou T B, Wang H, Ji S, et al. Soybean-derived mesoporous carbon as an effective catalyst support for electrooxidation of methanol[J]. Journal of Power Sources, 2014, 248: 427-433.

[30] Wang R F, Song H H, Li H, et al. Mesoporous nitrogen-doped carbon derived from carp with high electrocatalytic performance for oxygen reduction reaction [J]. Journal of Power Sources, 2015, 278: 213-217.

[31] Yi Q F, Zhang Y H, Liu X P, et al. Carbon-supported Fe/Co-N electrocatalysts synthesized through heat treatment of Fe/Co-doped polypyrrole-polyaniline composites for oxygen reduction reaction[J]. Science China-Chemistry, 2014, 57(5): 739-747.

[32] Lee J S, Park G S, Kim S T, et al. A highly efficient electrocatalyst for the oxygen reduction reaction: N-Doped ketjen black incorporated into Fe/$Fe_3C$-functionalized melamine foam[J]. Angewandte Chemie International Edition, 2013, 52(3): 1026-1030.

[33] Liang H W, Zhuang X, B S, et al. Hierarchically porous carbons with optimized nitrogen doping as highly active electrocatalysts for oxygen reduction[J]. Nature Communications, 2014, 5: 4973

[34] Wei W, Liang H W, Parvez K, et al. Nitrogen-doped carbon nanosheets with size-defined mesopores as highly efficient metal-free catalyst for the oxygen reduction reaction[J]. Angewandte Chemie International Edition, 2014, 53(6): 1570-1574.

[35] Liang J, Zheng Y, Chen J, et al. Facile oxygen reduction on a three-dimensionally ordered macroporous graphitic $C_3N_4$/carbon composite electrocatalyst[J]. Angewandte Chemie International Edition, 2012, 51(16): 3892-3896.

[36] Liu Z, Nie H G, Yang Z, et al. Sulfur-nitrogen co-doped three-dimensional carbon foams with hierarchical pore structures as efficient metal-free electrocatalysts for oxygen reduction reactions[J]. Nanoscale, 2013, 5(8): 3283-3288.

[37] Tucker J B. Amaranth -the once and future crop[J]. Bioscience 1986, 36(1): 9-13.

[38] Zhang W, Sherrell P, Minett A I, et al. Carbon nanotube architectures as catalyst supports for proton exchange membrane fuel cells[J]. Energy & Environmental Science, 2010, 3(9): 1286-1293.

[39] Zhang W, Sherrell P, Minett A I, et al. Carbon nanotube architectures as catalyst supports for proton exchange membrane fuel cells[J]. Energy & Environmental Science,

2010, 3(9): 1286-1293.

[40] Yang S B, Feng X L, Ivanovici S, et al. Fabrication of graphene-encapsulated oxide nanoparticles: Towards high-performance anode materials for lithium storage[J]. Angewandte Chemie International Edition, 2010, 49(45): 8408-8411.

[41] Chen P, Wang L K, Wang G, et al. Nitrogen-doped nanoporous carbon nanosheets derived from plant biomass: An efficient catalyst for oxygen reduction reaction[J]. Energy & Environmental Science, 2014, 7(12): 4095-4103.

[42] Liu Q, Zhang H Y, Zhong H W, et al. N-doped graphene/carbon composite as non-precious metal electrocatalyst for oxygen reduction reaction[J]. Electrochimica Acta, 2012, 81: 313-320

[43] Wang R F, Wang H, Zhou T B, et al. The enhanced electrocatalytic activity of okara-derived N-doped mesoporous carbon for oxygen reduction reaction[J]. Journal of Power Sources, 2015, 274: 741-747.

[44] Xiao M L, Zhu J B, Feng L G, et al. Meso/macroporous nitrogen-doped carbon architectures with iron carbide encapsulated in graphitic layers as an efficient and robust catalyst for the oxygen reduction reaction in both acidic and alkaline solutions[J]. Advanced Materials, 2015, 27 (15): 2521-2527.

# Recycling MF Solid Waste into Mesoporous Nitrogen-Doped Carbon with Iron Carbide Complex in Graphitic Layers as an Efficient Catalyst for Oxygen Reduction Reaction

ZHAO Can-yun[1,2], HUANG Lin[1,2,3], YOU Yong[1,2], YAO Ying-fang[1,2,3], SU Xiao-gang[1,2], WAN Hong[1,2], LIU Jian-guo[1,2,3,4*], WU Cong-ping[1,2,3]

(1. *College of engineering and Applied sciences, Nanjing University, Nanjing* 210093, *China*;
2. *Eco-materials and Renewable Energy Research Center, Nanjing University, Nanjing* 210093, *China*;
3. *Kunshan Innovation Institute of Nanjing University, Kunshan* 215347, *Jiangsu, China*;
4. *Suzhou High-tech Institute of Nanjing University, Suzhou* 215123, *Jiangsu, China*)

**Abstract:** Nitrogen-doped carbon materials with iron ions are known as catalytic growth agents for the oxygen reduction reaction (ORR) in fuel cells, but the design and synthesis of high-performance and low-cost catalysts still remain a significant challenge. Herein, we present a cost-effective approach to dispose of MF solid waste as the precursor for the synthesis of MCFes catalyst with the favorable structure features such as the high specific surface area, abundant active sites and suitable pore structure. The results showed that the MCFe-10/10/2had specific surface area as high as 780.7 $m^2 \cdot g^{-1}$ and high efficient catalytic activity comparable to commercial 5% Pt/C catalyst for the ORR in acid media. Furthermore, the influences in the contents of N through heat-treated at $NH_3$ atmosphere were also investigated in detail. It was found that the catalytic activity was sensitive to N type, particularly the ratio of pyridinic-N to total N atoms. The large N contents did not lead to higher ORR activities ofMCFes and NMCFe-10/10/2. While the pyridinic N content improved the onset potential for ORR. Furthermore, iron carbide nanoparticles were well encapsulated in N-doped graphene-like layers, which determined the limiting current density. This judicious transformation of organic-rich waste not only addresses the disposal issue, but also generates valuable functional carbon materials from the discard. The as-synthesized carbon will certainly have greater economic ramifications by creating value added materials from wastes.

**Key words:** melamine-formaldehyde; proton exchange membrane fuel cell; oxygen reduction reaction; FeN*x*/C; catalyst; waste utilization